Mid to late Holocene sea-level rise and precipitation variability recorded in the fringe mangroves of the Caribbean coast of Panama.

Carlos Castañeda-Posadas[1,2], Alex Correa-Metrio[2,3*], Jaime Escobar[4,5], J. Enrique Moreno[5], Jason Curtis[6], Maarten Blaaw[7], and Carlos Jaramillo[5]

[1] *Posgrado en Ciencias Biológicas, Universidad Nacional Autónoma de México, Coyoacán, Ciudad de México 04510, Mexico.*

[2] *Instituto de Geología, Universidad Nacional Autónoma de México, Coyoacán, Ciudad de México 04510, Mexico.*

[3] *Centro de Geociencias, Universidad Nacional Autónoma de México, Juriquilla, Querétaro 76230, Mexico.*

[4] *Departamento de Ingeniería Civil y Ambiental, Universidad del Norte, Barranquilla, Colombia.*

[5] *Center for Tropical Paleoecology and Archaeology, Smithsonian Tropical Research Institute, Box 0843-03092, Balboa, Panama.*

[6] *Department of Geological Sciences, University of Florida, Gainsville, FL 32611, United States of America.*

[7] *School of Natural and Built Environment, Queen's University Belfast, Belfast BT7 1NN, United Kingdom.*

* Corresponding author: acorrea@geociencias.unam.mx

Abstract

Throughout the Holocene, two of the most important factors involved in the evolution of tropical coastlines have been fluctuations in sea level and regional climates. The geological record provides insightful realizations of the complex interaction between these two factors, improving our understanding of the evolution of littoral zones. Here we present the sedimentary record of a mangrove swamp located in Punta Galeta, Caribbean coast of Panama. Through the conjunction of geochemical and biological sedimentary indicators, we reconstruct environmental dynamics of the area for the last ~5200 years. Between ~5200 and ~1800 cal yr B.P., the progressive dominance of carbonates and a decrease of mangrove pollen indicate increasing marine influence in the area, probably facilitated by a progressively drier climate. Between 3100 and 1800 cal yr B.P., the embayment was flooded by marine water resulting in a landward migration of mangroves. From ~1800 cal yr B.P. to present, the pollen and organic matter records indicate that mangrove vegetation belt recovered, contributing a large proportion of organic matter to the sediment and advancing the shoreline seaward. The maturation of the mangrove forest has resulted in a progradation process that offsets between 4 and 5 meters of sea level rise occurred through the last ~5000 years. This process was facilitated by the progressive decrease in rates of sea level rise and by increasing sedimentation rates resulting from a higher accumulation of organic matter from the more vigorous vegetation and more terrigenic input associated with higher regional precipitation. The record of Punta Galeta demonstrates that the evolution of fringe mangroves throughout the Holocene has been mostly driven by sea level rise, which effects are potentially offset by erosion during times of high precipitation. Thus, across the Caribbean coast, precipitation regimes have played a pivotal role at defining the structure and function of mangrove communities.

Keywords

Mangroves; sea level rise; precipitation variability; Caribbean; pollen analysis; geochemical analysis; Holocene.

1. Introduction

Regional coastal dynamics are defined by the differential strength of continental and marine influences that act upon a specific area (Bird, 2011). The local geomorphology and the balance between continental and marine influences define the physiognomy and complexity of the resulting ecosystems, which range from coastal dune fields to exuberant mangrove forests (Alongi, 2020; Ellison, 2004). These ecosystems intermediate the interchange of matter and energy between continental and marine areas and largely define the physiognomy of the coastlines (Alongi, 2020). Continental influences are mostly represented by the input of a mixture of materials of minerogenic and organic origin, transported mostly by rain and wind or produced *in situ*. Thus, these influences are mainly dominated by regional climates and the nature of the depositional environments. Marine influences, on the other hand, manifest through the erosive action of the waves and tides, and the control that sea level exerts on the hydraulic and compositional properties of the coastal soils. Through the Holocene, regional climates of Central America and sea level in the Caribbean have been variable (e.g. Khan et al., 2017; Stansell et al., 2020; Toscano and Macintyre, 2003; Winter et al., 2020), resulting a dynamic coastal landscape where ecosystems have been in a constant process of reconfiguration. Regional precipitation regimes, and thus sediment transport, have varied at time-scales from annual (e.g. interannual varibility of the Pacific system, Conroy et al., 2008) to millennial (e.g. the progressive southern dispalcement of the intertropical convergence zone, ITCZ, Haug et al., 2001). Sea level, on the other hand, has been rising at a progressively lower rate through time, reaching relatively stable levels between ~6000 and 5000 cal yr B.P. (Khan et al., 2017; Lambeck et al., 2014; Toscano and Macintyre, 2003). Thus, the modern landforms and ecosystems are the result of a dynamic evolutive history highly dependent on local and regional conditions.

Mangrove forests are probably the most exuberant ecosystem established in the intertidal zone of tropical and subtropical regions, in settings usually protected from the direct action of the waves (Lugo and Snedaker, 1974). Classified among the most productive ecosystems in the world, mangrove forests offer goods and services such as protection of the coastline from extreme weather events, storage of carbon, shelter for marine and terrestrial fauna, among others (Ward et al., 2016). During times of marine transgressive events such as the Holocene, their persistence over a given location largely depends on the input of lithogenic and organic materials offsetting sea level rise (Jaramillo and Bayona, 2000; Soares, 2009), a process facilitated by high precipitation regimes that associate with high erosion rates. Whereas sea level rises, mangroves facilitate terrain accretion and promote progradation processes, which are only possible given a reasonable input of sediments (Woodroffe, 1993). Thus, Holocene dynamics of mangroves provide hints into their response to rising sea level, although the variability of the input of continental can be an important source of variability. In this sense, the development of mangroves along coastal settings characterized by the absence of major tributaries (fringe mangroves, Lugo and Snedaker, 1974) offers a natural laboratory to identify vegetation responses to rising sea level.

Fringe mangrove communities have long thrived behind beach ridges and in embayments of the Caribbean (Ellison, 2004). In Panama, Punta Galeta is a good example of a setting protected from the direct effect of the waves inhabited by mangroves since at least 7000 cal yr B.P. (Macintyre and Glynn, 1976). The communities is composed of four mangrove species (*Avicennia germinans*, *Conocarpus erectus*, *Laguncularia racemosa*, and *Rhizophora mangle*), each one adapted to specific conditions of salinity and soil hydric regime, in turn defined by local geomorphology and the spatial structure of the intertidal zone (Ellison, 2004; Lugo and Snedaker, 1974; Sousa et al., 2007). Given the absence of major fluvial discharge into the area, mangrove dynamics through the Holocene have probably been largely dominated by sea level rise. We reconstruct the local and regional environmental history by analyzing geochemical and biological indicators in a sediment core from an embayment. Our main goal is to identify the effects of progressive sea level rise on the composition and structure of local mangrove communities, and the possible modulating role of regional climate. Whereas geochemical indicators provide insights on the environmental setting at local and regional spatial scales, palynological indicators provide independent evidence on local vegetation dynamics.

2. Study area

Punta Galeta is located on the Caribbean coast of central Panama, on the eastern side of the Panama Canal. It consists of a small peninsula surrounded by small islands (Fig. 1). The regional basement rock is part of the Gatun Formation, a middle and upper Miocene geological unit composed of massive siltstone to fine sandstone, and tuff, rich in molluscan fauna (Hendy, 2013; Woodring, 1957). The regional coastline is covered by deposits of marine carbonates that, in the Galeta coral reef, reach depths of at least 14 m (Macintyre and Glynn, 1976) (Fig. 1). Towards the embayments and behind the beach ridges, mangrove forests and swamps have developed, producing deposits rich in organic matter. The swamps are protected from direct wave action by a fringing reef flat that extends seaward, with its highest elevation in the fore reef and decreasing height landward (Kilar and Norris, 1988). The tidal regime is semidiurnal, with a mean diurnal range of 33.5 cm and a mean annual range of 21.3 cm (Cubit et al., 1986). Mean monthly temperature is relatively constant throughout the year, with an annual mean of 27.2 °C, and a daily temperature range of approximately 5 °C. Mean annual precipitation is ~2920 mm, with the dry season extending from January to mid-April (Fig. 1). The landward limit of the mangrove forests and swamps is determined by higher-elevation terrains occupied by tropical forest (Schmidt, 2008). The canopy of the mangrove forests of Punta Galeta is dominated by

Avicennia germinans (hereafter *Avicennia*), *Laguncularia racemose* (hereafter *Laguncularia*), and *Rhizophora mangle* (hereafter *Rhizophora*) (Sousa et al., 2007; Sousa and Mitchell, 1999). These species are distributed according to the tidal influence, forming zones of different canopy composition (Sousa et al., 2007). *Rhizophora* dominates the low intertidal areas, mixing with *Laguncularia* at distances of 10-20 m from the water's edge. *Avicennia* is present in the mid-intertidal areas, creating a canopy that has representatives of all three species. Additionally, there is sparse presence of *Conocarpus erectus* (hereafter *Conocarpus*), mostly found around the beach ridges and the transition zone from mangrove to tropical forest.

3. Methods

In October 2018, a 452-cm-long sediment core (GAL18) was retrieved from a mangrove forest in Punta Galeta, Caribbean coast of Panama (9.39°N 79.86°W, Fig. 1). The core was recovered in 1-m-long increments, using a modified Livingstone piston corer (Colinvaux et al., 1999), under a stand of *Avicennia germinans*. After retrieval, the core was sealed and has been stored at ~4 °C for preserving sedimentary evidence. Core sections were longitudinally open, and the material was photographed and described in terms of color, texture, and content of macro rests. Six depths along the core were sampled for radiocarbon dating on organic matter at the ^{14}CHRONO Centre for Climate, the Environment and Chronology of Queen's University Belfast. Radiocarbon dates were calibrated using IntCal20 (Reimer et al., 2020), expressed in calibrated years before present (cal yr B.P. hereafter), and interpolated using clam to construct an age-depth model (Blaauw, 2010).

The core was sampled at 5-cm intervals for geochemical analyses, for a total of 88 samples. For this purpose, 3-cm^3 subsamples were oven-dried and ground using a mortar and a pestle. Concentrations of major and trace elements were determined using a handheld XRF analyzer, with three repeated measurements per sample, and expressed in ppm. Confidence intervals for each element in each sample were calculated using the mean and standard deviation of the triplicate measurements. Only elements that showed concentrations statistically different from zero and that showed significant variability throughout the record were included in further analyses. Samples were also analyzed for total carbon (TC), total inorganic carbon (TIC), total nitrogen (TN), and carbon and nitrogen isotopes ($\delta^{13}C$ and $\delta^{15}N$) in bulk organic matter. Total carbon and total nitrogen were measured using a Carlo Erba NA 1500 CNS elemental analyzer.

Total inorganic carbon was determined by acidification followed by coulometric titration using an AutoMate Prep Device coupled with a UIC 5014 CO_2 coulometer. Percent total organic carbon was calculated by subtraction of TIC from TC. Subsamples for carbon isotope analysis on bulk organic matter were pretreated with 2N HCl to remove carbonate and later washed with distilled water to remove chloride, prior to isotope measurement. Around 50 mg of carbonate-free sediment was loaded into tin sample capsules for stable carbon isotope measurement. Nonacidified samples were used for nitrogen isotopes. Combustion gases were carried in a helium stream through a Conflo II interface to a Thermo Electron DeltaV Advantage isotope ratio mass spectrometer. Carbon and nitrogen isotope data are reported in per mil (‰) and expressed in standard delta notation. Carbon isotopes ($\delta^{13}C_{org}$) are reported relative to VPDB and nitrogen isotopes are reported relative to AIR. A principal component analysis (Jolliffe, 1986) was used to evaluate relationships among elements through a correlation biplot. Sample scores across the principal components (PC) were used to summarize the total variability of the geochemical record through time. TOC/TN ratios were calculated for each sample aiming to assess relative contributions of terrestrial and aquatic organic matter to the sediment (Meyers, 2003).

The core was subsampled every ~8 cm for pollen analysis for a total of 54 samples. Samples were prepared using standard techniques (Faegri and Iversen, 1989) and gravimetrically separated for concentrating palynomorphs (Krukowski, 1988). Samples were analyzed under a transmitted light microscope at magnifications of 400x and 1000x. Because of very low pollen concentrations, palynomorphs were counted aiming to a pollen sum of 200 grains, which included pollen of terrestrial plants and spores of *Acrostichum,* as this taxon is considered a component of the vegetation in mangrove communities (Lee et al., 2017). Pollen from aquatic plants was excluded from the pollen sum because they are probably transported from freshwater streams that descend from the area occupied by the tropical forest. Pollen types were identified to the finest possible taxonomic level using available reference pollen collections and specialized literature (Bush and Weng, 2007; Roubik and Moreno, 1991; Willard et al., 2001). All palynomorph abundances were transformed to percentages of the pollen sum.

4. Results

4.1 Core stratigraphy and chronology

The core was characterized by two main sections differentiated by their texture and the presence of macrorests (Fig. 2). The lower section, from 452 to 250 cm below lagoon floor (blf hereafter), was characterized by abundant bivalve and gastropod shells, low content of organic matter, and a relatively coarse sediment texture dominated by lime and sand. The upper section, from 250 cm blf to the top of the core, was characterized by abundant vegetal macrorests, high content of organic matter, and a finer sediment texture dominated by lime and clay (Fig. 2). Radiocarbon dates resulted in stratigraphic order, except the sample taken at 331 cm blf that showed an age reversal and was, therefore, excluded from the age-depth model (Fig. 2). According to the age-depth model, the sediment sequence GAL18 spans the last ~5,200 years (Fig. 2). Sedimentation rate showed a general increase towards present, going from ~0.05 cm/yr from ~452 to 320 cm blf, to 0.2 cm/year in the uppermost ~100 cm of the record (Fig. 2).

Table 1. Radiocarbon and calibrated dates of core GAL18. 95% confidence intervals for calibrated ages are shown in parenthesis.

Laboratory ID	Depth (cm)	^{14}C Age	Error	Calibrated age (cal yr BP)
UBA-40771	45	138	23	136 (12-269)
UBA-40772	91	338	22	389 (317-469)
UBA-40773	195	1553	28	1441 (1363-1515)
UBA-40774	311	2269	25	2259 (2162-2340)
UBA-40935	330	892	20	2665 (2583-2737)
UBA-40776	435	4340	28	4908 (4850-4975)

4.2 Geochemical analyses

Concentrations of Ca, Cu, Fe, K, Mo, Mn, Rb, S, Sr, Ti, Zn, and Zr, determined by XRF analysis, were significantly different from zero and displayed significant variability through the record (Fig. 3). Mo, Cu, and Rb were characterized by stable concentrations from the bottom of the record to ~500 years cal yr B.P. Thereafter, concentrations increased, reaching a peak around 200 cal yr B.P. (Fig. 3). Fe, S, Ti, Zn, and Zr were characterized by relatively low and stable concentrations from the bottom of the record to ~2000 cal yr B.P. These elements showed higher and more variable values from ~2000 cal yr B.P. to the top of the core. K showed a long-term decreasing trend throughout the record, whereas Mn remained stable from the bottom of the record to ~2000 cal yr B.P., when it began to decrease towards present (Fig. 3). Ca and Sr increased from the bottom of the record to ~3100 cal yr B.P., reaching a plateau of maximum concentrations that lasted until ~2000 cal yr B.P. and subsequently decreasing towards present.

TC and TN were characterized by low and stable concentrations from the bottom of the sediment core to ~2000 cal yr B.P. (Fig. 3). $\delta^{13}C_{org}$ values were relatively stable (-24.0‰) and less negative from the bottom of the record to ~2000 cal yr B.P., when they started to decrease, reaching their most negative values in the topmost sample (-29.0‰) (Fig. 3). $\delta^{15}N$ was characterized by values around 2.0‰ between the bottom of the record and ~4000 cal yr B.P. Values increased to ~2.5‰ between 4000 and 1500 cal yr B.P., and thereafter decreased towards present.

In the PCA, more than half of the total variance of the dataset was associated with PC1 (Fig. 4). The broken-stick model indicates that only the two first principal components were statistically significant, representing 51.1% and 14.9% of the total variance, respectively (Fig. 4). The positive end of PC1 is associated with Ca, Mn, Sr, TIC, $\delta^{15}N$, and $\delta^{13}C_{org}$, whereas the negative end was associated with Cu, Mo, Rb, S, Ti, TN, TOC, and Zr (Fig. 4). PC2 was mostly defined by K and Zr towards the positive end, and Fe and Zn towards the negative end.

4.3 Palynological analysis

Pollen sums varied between 92 and 781 grains per sample (mean = 260, Q1 = 194 and Q3 = 293). Samples in which the pollen sum was below the target of 200 grains were mostly from below 330 cm blf. Pollen spectra were characterized by 57 morphotypes, 28 and 29 classified to genus and family levels, respectively. Counts of fern spores other than *Acrostichum* ranged from 5 to 65 spores per sample (mean = 26, Q1 = 14 and Q3 = 30), and were represented by the families Lycopodiaceae, Selaginellaceae, Aspleniaceae, Cyatheaceae, Polypodiaceae, and Pteridaceae. The most abundant taxa were *Rhizophora* (mean 36.4%), *Avicennia* (17.6%), *Achrostichum* (11.7%), cf. *Laguncularia* (6.9%), *Polypodium* (4.7%), *Bombacopsis* (4.5%), *Cecropia* (4.3%), *Asplenium* (3.3%), Cyatheaceae (2.2%), Urticaceae-Moraceae (2.0%), Poaceae (1.75%), and Arecaceae (1.6%) (Fig. 5). See full diagram in Appendix 1 of Supplementary Material.

In the fossil pollen spectra, mangroves were represented by *Avicennia*, cf. *Laguncularia*, and *Rhizophora*, with sporadic appearances of *Conocarpus* (Fig. 5). *Acrostichum* spores were also an important component of the palynomorph counts, with higher percentages before 2000 cal yr B.P. Herbs were mostly represented by Urticaceae-Moraceae, *Chenopodium*, and Amaranthaceae that better represented in samples older than ~3800 cal yr B.P. (Fig. 5). Aquatics were represented by Cyperaceae, *Nymphea*, and *Polygonum* (Fig. 5). Other herbs such as *Ambrosia* and *Polygala* were more abundant between ~3100 and 1500 cal yr B.P., whereas the last 2000 years were characterized by relatively high abundances of *Mimosa* and Asteraceae (Fig. 5). Trees and shrubs were present throughout the entire record, although their abundances were higher between 3100 and 1800 cal yr B.P. *Alnus* and *Podocarpus* were more abundant in samples older than 3000 cal yr B.P.

5. Discussion

Core GAL18 spans the last 5,200 years of the environmental history of Punta Galeta, Caribbean coast of Panama (Fig. 2). Sedimentation rates resulted variable and were punctuated by radiocarbon dates, implying that our age-depth model offers a rough approximation to the temporal structure of the environmental history of the area during the last 5,200 years. Further, the age-depth model must be interpreted in the light of a possible influence of old carbon, an important source of chronological overestimation under environments with high marine influence (Stuiver and Braziunas, 1993). Low sedimentation rates below 311 cm blf (before ~2200 cal yr B.P.) could be reflecting a depositional hiatus previously reported for the area (Schmidt, 2008) that roughly coincides with a drought reported for several coastal sites in the Caribbean and surrounding regions (e.g. Giry et al., 2012; Haug et al., 2001; Stansell et al., 2020; Velez et al., 2014). Differences in sediment composition and sedimentation rates between the lower and upper part of the core reflect concomitant changes of both the depositional environment and regional climatic conditions. Whereas depositional environments in costal settings such as Punta Galeta show high spatiotemporal variability (Woodroffe, 1993), Holocene changes in precipitation regime and human activities have been documented for the region (e.g. Correa-Metrio et al., 2016; Piperno et al., 1991; Toth et al., 2015). In the following sections, we first introduce the interpretation of the proxies analyzed for core GAL18 and then, present an interpretation of the environmental history of the area.

5.1 Geochemical indicators

The composition of the sediments of core GAL18 reflects the balance between continental and marine influences that define sediment sources as well as transport and deposition patterns. The continental influence is associated with the input of detrital materials eroded from the catchment basin. Punta Galeta lies on the Gatun Formation, a shallow marine sequence rich in carbonates and in siliciclastic material of volcanic origin (Hendy, 2013; Hidalgo et al., 2011). Thus, in our geochemical dataset, the continental influence is surely represented by lithogenic elements such as Rb, Ti, and Zr, which concentrations reflect the dynamics of the erosive agents (Boës et al., 2011; Rothwell and Croudace, 2015). Carbonates eroded from the basin probably represent a substantial source of TIC and Ca, but the negative association of these elements with lithogenics (Fig. 4) points to marine carbonates as their main source at the coring location. TIC and Ca are strongly correlated with Mn and Sr, and $\delta^{13}C_{org}$ (Figs. 3 and 4), reinforcing the interpretation of their association with marine sources as marine organic matter carbon is isotopically heavier (Meyers, 1997; Schneider et al., 2006). High concentrations of Ca, Sr, and TIC accompanied by less negative values of $\delta^{13}C_{org}$ are probably associated with subtidal depositional environments where large amounts of marine carbonates precipitate. Overall, the main variability of the geochemical record was reflected by the trends of two groups of correlated elements: one associated with input of detrital material and the other associated with deposition of marine carbonates (Figs. 3 and 4).

Accumulation of organic matter in the sediments is directly reflected by concentrations of TOC (Meyers, 2003). In core GAL18, the positive correlation between concentrations of TOC, S and Mo (Figs. 3 and 4) indicate organic matter that has accumulated under poorly oxygenated conditions that inhibit oxidative processes. Under a reduced depositional environment, concentrations of Mo increase because of its lower mobility (Smedley and Kinniburgh, 2017), whereas bacterial activity favors the accumulation of S (Goldhaber, 2003). High concentrations of Fe and Zn usually indicate oxygen availability (Tribovillard et al., 2006), but these elements can also associate with the organic fraction of the sediment (Dean et al., 1997). Towards the upper part of our record, concentrations are of Fe and Zn are in phase with those of TOC and Cu (Fig. 3), suggesting that, in our record, these elements associate with changes in organic matter productivity. The peaks of these elements that characterize the upper part of the record coincide with substantial decreases of $\delta^{15}N$ (Fig. 3), which were probably associated with denitrification caused by high bacterial activity under anoxic conditions (Hodell and Schelske, 1998).

PC1 indicates that the main mode of variability in core GAL18 is associated with changes in the balance between terrigenic and marine sediments, and thus with the balance between continental and marine influences in the area. While the negative end of the axis reflects substantial input of organic matter and lithogenic elements (mainly Rb, Ti, and Zr), the positive end is defined by elements associated with marine carbonates (mainly Ca, TIC, and Sr). Dominant deposition of terrigenic materials indicated by negative scores along PC1 probably took place under inter to supratidal environments. On the other hand, dominant deposition of marine carbonates indicated by positive scores of PC1 probably took place under inter to infratidal environments. PC2, on the other hand indicates a mode of variability probably associated with the dominant sources of terrigenic material (lithogenic vs. organic) and with oxygen availability in the water column. Whereas the positive end of PC2 was mostly defined by K, Ti, and Zr (Fig. 4), all lithogenic conservative elements (Boës et al., 2011; Rothwell and Croudace, 2015), the negative end was defined by Cu, Zn, and Fe, which associate with organic matter and/or with oxygen availability in the depositional environment (Dean et al., 1997; Tribovillard et al., 2006). The association of these elements with TOC indicates that the negative end of PC2 is more related to the accumulation of organic matter.

5.2 Biological indicators

The pollen assemblages deposited in the sediments of Punta Galeta are dominated by local components with mangrove taxa representing more than 40% of the pollen sum, as commonly found in mangrove sediments (Behling et al., 2001; Urrego et al., 2009). This overrepresentation pattern obscures the signal of pollen from trees and shrubs from the surrounding tropical forests, impeding a detailed interpretation of their variability though the record. On the other hand, the geomorphology of Punta Galeta offers very limited space for the formation of back swamps and saltmarshes (Sousa et al., 2007), hindering the development of a clear salinity-driven zonation of herbaceous taxa that characterize well-developed tidal flats (Behling et al., 2001; Urrego et al., 2009). Thus, herbaceous taxa in the sedimentary record of Punta Galeta probably reflect patterns of vegetation disturbance instead of changes in soil salinity. Most of taxa represented in the palynological record are associated with herbaceous vegetation and shrubs and trees from tropical forests, except for *Alnus* and *Podocarpus* that often associate with forests from higher elevations (Marchant et al. 2002). In core GAL18, however, these taxa occurred mostly in abundances below 1.5% probably resulting from long-distance transported pollen (Fig. 5). Overall, the variability of the pollen spectra from core GAL18 mostly reflects local vegetation dynamics. The progressive increase of pollen percentages from all mangrove taxa reflects the invigoration of this vegetation time through time. On the other hand, variability of individual mangrove taxa probably reflects changes in the spatial configuration of the community.

Through the last 5200 years, the most important pollen taxa of the mangrove of Punta Galeta have been *Avicennia*, cf. *Laguncularia*, and *Rhizophora*, coinciding with the taxa that dominate the modern canopy of the local mangrove forests (Sousa et al., 2007; Sousa and Mitchell, 1999). The sporadic appearance of pollen of *Conocarpus* coincides with the minor representation of this taxon in the modern vegetation (Schmidt, 2008). Contrastingly, whereas *Acrostichum* is a relatively minor component of the modern forests, it seems to have been better represented from the bottom of the record to ~700 cal yr B.P. (Fig. 5). Given the association of this fern with rather sparse canopies (Medina et al., 1990), it is possible that this time period were characterized by a more sparse mangrove canopy. In fact, from ~5000 to 2000 cal yr B.P., percentages of *Rhizophora* were relatively low (between ~21 and 32%, Fig. 5), considering the usual over-representation of this taxa in pollen spectra (e.g. Behling et al., 2001; Ramcharan and McAndrews, 2006; Urrego et al., 2009). The coincidence of rising percentages of *Rhizophora* and cf. *Laguncularia* through the last 2000 years likely indicates that the mangrove vegetation that occupies Galeta today is a relatively novel community in the context of the last 5000 years. From 5200 to 5000 cal yr B.P., percentages of *Rhizophora* and cf. *Laguncularia* were relatively high, although the higher abundances of *Avicennia* suggest a mangrove community with a structure different than that of today.

5.3 Environmental turnover in Punta Galeta through the last ~5200 years

During the last 5200 years, the environmental variability of Punta Galeta has been largely associated with the marine transgression that has characterized coastal settings during the Holocene. Regional climatic variability at interannual to millennial scale seem to have played an important role at amplifying the effects of sea-level rise on the mangroves of Punta Galeta. Thus, our record provides insights into the response of the shoreline to the rising sea level and the progradation process mediated by the mangrove community, constituting a typical sedimentary parasequence (*sensu* Catuneanu and Zecchin, 2020). The general variability pattern is summarized by the PCA, with PC1 representing the balance between continental and marine influences on the depositional processes, and PC2 indicating the dominating nature of the terrigenic sediments. The palynological record, on the other hand, reflects the local dynamics of the mangrove forests in response to the geomorphological dynamics associated with sea level rise and regional precipitation changes. Based on the geochemical and biological evidence, we divide the history of the area into four main environmental stages. This discretization of the record does not intend to provide a formal chronostratigraphy, but rather to facilitate the interpretation of environmental variability in the area. Stage I (from 5200 to 5000 cal yr B.P.) represents a depositional environment under supra to intertidal conditions covered by a mature mangrove forest. Stage II (from ~5000 to 3100 cal yr B.P.) represents a inter tidal environment submitted to a progressively higher water column, and probably progressively dryer conditions. Rapidly increasing sea level rise and likely lower precipitation led to Stage III, characterized by infratidal conditions that lasted from ~3100 to 1800 cal yr B.P. From 1800 cal yr B.P. to present, the coring site was characterized by a rapid infilling, first with terrigenic materials that probably reflect a precipitation rebound (Stage IV, from ~1800 to 700 cal yr B.P.) followed by organic matter (Stage V, 700 cal yr B.P. to modern).

Stage I. (~5200 to 5000 cal yr B.P.). The lowermost 200 years of the record were characterized by mangrove pollen percentages above 70%, with equitable representation of *Rhizophora*, *Avicennia*, and cf. *Laguncularia* (Fig. 6), suggesting a well-established mangrove community. The coring site was probably on the distal part of the coastline, which was migrating landward given the progressive sea level rise that has characterized the Caribbean throughout the Holocene (Toscano and Macintyre, 2003). High concentrations of TOC through these 200 years (Fig. 6) indicate a relatively stable substratum with accumulation of organic matter. Percentages of mangrove taxa above 60% (Fig. 6) suggest that the coring site was occupied by a mangrove forest located towards the upper limit of the tidal range. PC1 sample scores indicate an intertidal depositional environment, whereas PC2 indicates high deposition of organic matter that, according to C/N ratios above 20, was mostly derived from terrestrial vegetation (Meyers, 2003; Rovai et al., 2018). Relatively high precipitation that coincides with a more northerly position of the Intertropical Convergence Zone (Haug et al., 2001) probably played a significant role at maintaining a vigorous vegetation. Low concentrations of lithogenics probably result from the high concentration of organic matter in the sediment.

Stage II (~5000 to 3100 cal yr B.P.). A substantial decrease of mangrove pollen at ~5000 cal yr B.P. indicates a sparser mangrove stand. Increasing PC1 scores indicate a progressive increase of marine influence in the area (Fig. 6), whereas decreasing concentrations of lithogenics (Fig. 3) indicate a long-term trend towards drier conditions. Sedimentation rates were exceeded by rates of sea level rise (Fig. 6), resulting in a progressive flooding of the coring site and thus a higher precipitation of marine carbonates. Decreasing concentrations of lithogenics indicate a trend towards drier conditions that coincides with an invigoration of the drying trend reported for the Northern Hemisphere through the Holocene based on the record of Cariaco Basin (Haug et al., 2001; Winter et al., 2020). Mangrove forests responded to this sea level rise process by migrating landward, thus becoming sparser at the coring site. Higher abundances of *Acrostichum* indicate a sparser canopy as this fern usually associates with disturbed mangrove forests (Medina et al., 1990). PC2 indicates that terrigenic sediments were mostly lithogenic, which reflects on the decreasing concentrations of TOC. Less negative $\delta^{13}C_{org}$ and C/N ratios between 16 and 18 indicate a higher contribution of marine phytoplankton to the organic matter (Meyers and Lallier-vergès, 1999; Meyers, 2003). TOC values are, indeed, similar to those reported for river deltas (Rovai et al., 2018) where substrate is relatively unstable. The deepening of the lagoon together with the more open vegetation probably increased the energetic impact of the tides around the coring location.

Stage III (~3100 to 1800 cal yr B.P.). Percentages of mangrove pollen ~40% indicate that the forest around the coring site was still sparse (Figs. 5 and 6). This period was characterized by less negative $\delta^{13}C_{org}$ values that indicate organic matter production was dominated by marine phytoplankton (Meyers and Lallier-vergès, 1999), and C/N ratios below 15 that are characteristic of estuarine systems of brackish water (Rovai et al., 2018). High and stable values of PC1 indicate strong marine influence characterized by high concentration of carbonates, most likely deposited under an infratidal environment. According to PC2, the terrigenic fraction became progressively more organic, although high concentrations of Mn and increasing concentrations of Fe and Zn indicate a well oxygenated water column (Tribovillard et al., 2006). These negative PC2 scores are also related to the lowest concentrations of lithogenics throughout the record, which could be indicating a relatively dry regional climate. Dry conditions have been reported for other location in Central America and the western Atlantic during this time (Giry et al., 2012; Stansell et al., 2020; Velez et al., 2014), suggesting a regional driver of precipitation variability. According to evidence from the Galapagos Islands, El Niño events were frequent between ~4000 and 1500 cal yr B.P. (Conroy et al., 2008), which probably increased precipitation seasonality in Punta Galeta. This time interval was also reportedly characterized by La Niña-like conditions (Toth et al., 2015), which in Panama result in a higher precipitation variability (Fig. 1C). The conjunction of El Niño and La Niña were likely associated with a higher both seasonality interannual variability of precipitation, offering a plausible scenario for the low deposition of lithogenic elements. Nevertheless, the high uncertainty of our age-depth model precludes definite conclusions on the effect of the ENSO system on the climate and vegetation of Punta Galeta. Additionally, decreasing PC2 scores coincide with a gradual southern displacement of the ITCZ (Haug et al., 2001), which would associate with lower mean annual precipitation (Fig. 6). Higher percentages of Arecaceae, Fabaceae, and Malvaceae (Fig. 5) offer further evidence of a relatively high precipitation seasonality. Increasing percentages of *Ambrosia* suggest anthropogenic influence, widely documented for Central Panama through this time interval (Cooke and Ranere, 1992; Piperno, 2006; Piperno et al., 1991), could have acted as an additional source of pressure on vegetation. The evidence suggests that, during this stage, the water column in Punta Galeta reached its maximum levels through the last ~5200 years, leaving the coring site in the subtidal zone. These conditions indicate that rising sea level rates exceeded the accretion rates that were diminished because of the low sediment input from pluvial erosion.

Stage IV (~1800 to 700 cal yr B.P.). Increasing percentages of mangrove taxa and TOC concentrations indicate a recovery of mangrove vegetation accompanied by a monotonic trend of organic carbon accumulation in the soil (Figs. 5 and 6). The increasing trend of PC1 scores suggest a progressive increase of terrestrial influence (Fig. 6). Higher concentrations of lithogenic elements summarized by the increasing scores of PC2 indicate a rebound of moisture availability, which could be associated with higher sedimentation rates. Even though El Niño events were still frequent (Conroy et al., 2008; Moy et al., 2002), the change in the hydroclimate probably resulted from two main factors, both of them associated with lower seasonality: i) the termination of the La Niña-like conditions (Fig. 6) (Toth et al., 2015), and ii) a decrease of insolation seasonality driven by increasing insolation through the moths of higher moisture deficit (January to April, Figs. 1 and 6). This trend towards wetter conditions has also been reported for the Galapagos Islands (Conroy et al., 2008), highlighting the importance of the Pacific system at modulating moisture availability patterns of Central Panama (Correa-Metrio et al., 2016). Sedimentation rates increased over the rate of sea level rise, diminishing the depth of the water column, leaving the coring site in the intertidal zone. The stage represents a seaward progradation the terrain facilitated by increasing sedimentation rates, in turn associated with a higher terrigenic input of sediments and a more vigorous mangrove.

Stage V (~700 cal yr B.P. to Present). The mangrove vegetation through this stage was characterized by increasing percentages of cf. *Laguncularia* (Fig. 6). This taxon in Galeta represents the transition between the waterfront dominated by *Rhizophora* and the stands of *Avicennia* that dominate the upper inter-tidal areas (Sousa et al., 2007). This stage probably corresponds to the establishment of the modern mangrove forest with a well-developed zonation of taxa. Whereas $\delta^{13}C$ and C/N values suggest that organic matter is mostly contributed by terrestrial plants (Meyers, 2003), the latter values are characteristic of mangrove forests located on carbonate settings (Rovai et al., 2018). The regional vegetation resulted enriched with Annonaceae, Araceae, *Cecropia*, *Machaerium*, and Rubiaceae, suggesting a more diverse forest. Although highly variable, PC1 scores reach their lowest values indicating high terrestrial influence, which, according to PC2 consists mostly of organic matter (Fig. 6). Towards the upper part of the stage, sea level rise rates for the Caribbean and sedimentation rates at Punta Galeta equilibrate, coinciding with the highest accumulation of organic carbon in the soil (Fig. 6).

6. Conclusions

The development of mangrove communities is the result of an intricate network of interactions between local and regional factors. In the Caribbean coast of Panama, sea level has defined the baselines for erosion and deposition, whereas regional precipitation has been linked to sedimentary input and vegetation vigor. The interaction between these two main factors defines sediment accumulation and soil accretion, as well as substrate salinity, all of them in turn associated with vegetation composition and structure. The sedimentary record of Punta Galeta demonstrates that the monotonically increasing sea level of the Caribbean has played a major role at defining the establishment of fringe mangroves in the area. According to the geochemical evidence, more than half of the local environmental variability (50.3% of the variance reflected in PC1) has been directly linked to the depositional processes, which reflects the balance the between marine and terrestrial influences. The balance between these two sources of variability defined the spatiotemporal distribution of the mangrove community, which from ~5200 to 1800 cal yr B.P. migrated landward, and from 1800 cal yr B.P. to present have led a seaward progradation of the terrain. PC2 reflets a secondary mode of environmental variability reflected in the main composition of the terrigenic fraction of the sediments probably associated with precipitation variability. Through the last 5200 years, there has been a trend towards lower concentrations of lithogenic conservative elements, indicating a trend towards drier conditions and coinciding with the southward displacement of the intertropical convergence zone (Haug et al., 2001). More important, however, has been the variability related to the ENSO system, with high El Niño frequency associated with high precipitation variability. Overall, the establishment and thriving of mangrove forests has been a result of the equilibrium between rates of sea level rise and rates of soil accretion. Well-established mangroves coincided with the highest accumulation of TOC, highlighting the importance of mangrove vegetation for maintaining soil carbon stocks.

Acknowledgments.

This study has been performed in partial fulfillment of the requisites of the *Posgrado en Ciencias Biológicas*, UNAM, for the Ph.D. degree of C.C.-P. Financial support from UNAM-DGAPA grant IN208819.We are grateful to Luis Gerardo Martínez and Astrid Salgado for their assistance with the XRF analysis, and to Sara Solís for her support with the lab work.

References

Alongi, D.M., 2020. Coastal ecosystem processes. CRC press.

Behling, H., Cohen, M.C.L., Lara, R.J., 2001. Studies on Holocene mangrove ecosystems dynamics of the Braganca Peninsula in north-eastern Para, Brazil. Palaeogeography, Palaeoclimatology, Palaeoecology 167, 225-242.

Bird, E.C., 2011. Coastal geomorphology: an introduction. John Wiley & Sons.

Blaauw, M., 2010. Methods and code for 'classical'age-modelling of radiocarbon sequences. Quaternary Geochronology 5, 512-518.

Boës, X., Rydberg, J., Martinez-Cortizas, A., Bindler, R., Renberg, I., 2011. Evaluation of conservative lithogenic elements (Ti, Zr, Al, and Rb) to study anthropogenic element enrichments in lake sediments. Journal of Paleolimnology 46, 75-87.

Bush, M.B., Weng, C., 2007. Introducing a new (freeware) tool for palynology. Journal of Biogeography 34, 377-380.

Catuneanu, O., Zecchin, M., 2020. Parasequences: Allostratigraphic misfits in sequence stratigraphy. Earth-Science Reviews, 103289.

Colinvaux, P., de Olivera, P.E., Moreno, P.J.E., 1999. Amazon Pollen Manual and Atlas. Harwood Academic Publishers, Amsterdam.

Conroy, J.L., Overpeck, J.T., Cole, J.E., Shanahan, T.M., Steinitz-Kannan, M., 2008. Holocene changes in eastern tropical Pacific climate inferred from a Galápagos lake sediment record. Quaternary Science Reviews 27, 1166-1180.

Cooke, R., Ranere, A.J., 1992. Prehistoric human adaptations to the seasonally dry forests of Panama. World Archaeology 24, 114-133.

Correa-Metrio, A., Vélez, M.I., Escobar, J., St-Jacques, J.-M., López-Pérez, M., Curtis, J., Cosford, J., 2016. Mid-elevation ecosystems of Panama: future uncertainties in light of past global climatic variability. Journal of Quaternary Science 31, 731-740.

Cubit, J.D., Windsor, D.M., Thompson, R.C., Burgett, J.M., 1986. Water-level fluctuations, emersion regimes, and variations of echinoid populations on a Caribbean reef flat. Estuarine, Coastal and Shelf Science 22, 719-737.

Dean, W.E., Gardner, J.V., Piper, D.Z., 1997. Inorganic geochemical indicators of glacial-interglacial changes in productivity and anoxia on the California continental margin. Geochimica et Cosmochimica Acta 61, 4507-4518.

Ellison, A.M., 2004. Wetlands of central America. Wetlands Ecology and Management 12, 3-55.

Faegri, K., Iversen, J., 1989. Textbook of pollen analysis, 4th ed. Wiley, Chichester.

Giry, C., Felis, T., Kölling, M., Scholz, D., Wei, W., Lohmann, G., Scheffers, S., 2012. Mid-to late Holocene changes in tropical Atlantic temperature seasonality and interannual to multidecadal variability documented in southern Caribbean corals. Earth and Planetary Science Letters 331, 187-200.

Goldhaber, M.B., 2003. Sulfur-rich sediments, in: Holland, H.D., Turekian, K.K. (Eds.), Treatease of Geochemistry. Elsevier, pp. 257-288.

Haug, G.H., Hughen, K.A., Sigman, D.M., Peterson, L.C., Rohl, U., 2001. Southward migration of the Intertropical Convergence Zone through the Holocene. Science 293, 1304-1308.

Hendy, A.J., 2013. Spatial and stratigraphic variation of marine paleoenvironments in the middle-upper Miocene Gatun Formation, Isthmus of Panama. Palaios 28, 210-227.

Hidalgo, P.J., Vogel, T.A., Rooney, T.O., Currier, R.M., Layer, P.W., 2011. Origin of silicic volcanism in the Panamanian arc: evidence for a two-stage fractionation process at El Valle volcano. Contributions to Mineralogy and Petrology 162, 1115-1138.

Hodell, D.A., Schelske, C.L., 1998. Production, sedimentation, and isotopic composition of organic matter in Lake Ontario. Limnology and Oceanography 43, 200-214.

Jaramillo, C., Bayona, G., 2000. Mangrove Distribution during the Holocene in Tribugá Gulf, Colombia 1. Biotropica 32, 14-22.

Jolliffe, I.T., 1986. Principal Component Analysis. Springer-Verlag, Berlin.

Khan, N.S., Ashe, E., Horton, B.P., Dutton, A., Kopp, R.E., Brocard, G., Engelhart, S.E., Hill, D.F., Peltier, W., Vane, C.H., 2017. Drivers of Holocene sea-level change in the Caribbean. Quaternary Science Reviews 155, 13-36.

Kilar, J.A., Norris, J.N., 1988. Composition, export, and import of drift vegetation on a tropical, plant-dominated, fringing-reef platform (Caribbean Panama). Coral Reefs 7, 93-103.

Krukowski, S.T., 1988. Sodium metatungstate; a new heavy-mineral separation medium for the extraction of conodonts from insoluble residues. Journal of Paleontology 62, 314-316.

Lambeck, K., Rouby, H., Purcell, A., Sun, Y., Sambridge, M., 2014. Sea level and global ice volumes from the Last Glacial Maximum to the Holocene. Proceedings of the National Academy of Sciences 111, 15296-15303.

Lee, S., Jones, E., Diele, K., Castellanos-Galindo, G., Nordhaus, I., 2017. Biodiversity, in: Rivera-Monroy, V.H., Lee, S., Kristensen, Y.E., Twilley, R.R. (Eds.), Mangrove Ecosystems: a Global Biogeographic Perspective. Springer, New York, NY, USA, pp. 55–86.

Lugo, A.E., Snedaker, S.C., 1974. The Ecology of Mangroves. Annual Review of Ecology and Systematics 5, 39-64.

Macintyre, I., Glynn, P., 1976. Evolution of modern Caribbean fringing reef, Galeta point, Panama. AAPG Bulletin 60, 1054-1072.

Marchant, R., Almeida, L., Behling, H., Berrio, J.C., Bush, M., Cleef, A., Duivenvoorden, J., Kappelle, M., de Oliveira, P., de Oliveira-Filho, A.T., Lozano-Garcia, S., Hooghiemstra, H., Ledru, M.-P., Ludlow-Wiechers, B., Markgraf, V., Mancini, V., Paez, M., Preto, A., Rangel, O., Salgado-Labouriau, M.L., 2002. Distribution and ecology of parent taxa of pollen lodged within the Latin American Pollen Database. Review of Palaeobotany and Palynology 121, 1-75.

Medina, E., Cuevas, E., Popp, M., Lugo, A.E., 1990. Soil salinity, sun exposure, and growth of Acrostichum aureum, the mangrove fern. Botanical Gazette 151, 41-49.

Meyers, P., Lallier-vergès, E., 1999. Lacustrine Sedimentary Organic Matter Records of Late Quaternary Paleoclimates. Journal of Paleolimnology 21, 345-372.

Meyers, P.A., 1997. Organic geochemical proxies of paleoceanographic, paleolimnologic, and paleoclimatic processes. Organic Geochemistry 27, 213-250.

Meyers, P.A., 2003. Applications of organic geochemistry to paleolimnological reconstructions: a summary of examples from the Laurentian Great Lakes. Organic Geochemistry 34, 261-289.

Moy, C.M., Seltzer, G.O., Rodbell, D.T., Anderson, D.M., 2002. Variability of El Niño/Southern Oscillation activity at millenial timescales during the Holocene epoch. Nature 420, 162-165.

Paton, S., 2019. Monthly summary Galeta Station. The Smithsonian Institution.

Piperno, D.R., 2006. Quaternary environmental history and agricultural impact on vegetation in central America. Annals of the Missouri Botanical Garden 93, 274-296.

Piperno, D.R., Bush, M.B., Colinvaux, P.A., 1991. Paleoecological perspectives on human adaptation in Panama. II: The Holocene. *Geoarchaeology*, 227-250.

Ramcharan, E.K., McAndrews, J.H., 2006. Holocene development of coastal wetland at Maracas bay, Trinidad, West Indies. Journal of Coastal Research 22, 581-586.

Reimer, P.J., Austin, W.E., Bard, E., Bayliss, A., Blackwell, P.G., Ramsey, C.B., Butzin, M., Cheng, H., Edwards, R.L., Friedrich, M., 2020. The IntCal20 Northern Hemisphere radiocarbon age calibration curve (0–55 cal kBP). Radiocarbon 62, 725-757.

Ropelewski, C.F., Jones, P.D., 1987. An extension of the Tahiti-Darwin southern oscillation index. Monthly Weather Review 115, 2161-2165.

Rothwell, R.G., Croudace, I.W., 2015. Twenty years of XRF core scanning marine sediments: what do geochemical proxies tell us?, in: Croudace, I.W., Rothwell, R.G. (Eds.), Micro-XRF Studies of Sediment Cores. Springer Netherlands, Dordrecht, pp. 25-102.

Roubik, D.W., Moreno, P.J.E., 1991. Pollen and Spores of Barro Colorado Island. Monographs in Systematic Botany 36, Missouri Botanical Garden.

Rovai, A.S., Twilley, R.R., Castañeda-Moya, E., Riul, P., Cifuentes-Jara, M., Manrow-Villalobos, M., Horta, P.A., Simonassi, J.C., Fonseca, A.L., Pagliosa, P.R., 2018. Global controls on carbon storage in mangrove soils. Nature Climate Change 8, 534-538.

Schmidt, D.P., 2008. A palynological and stratigraphic analysis of mangrove sediments at punta galeta, panama. University of California, Berkeley, Berkeley.

Schneider, R.R., Schulz, H.D., Hensen, C., 2006. Marine carbonates: their formation and destruction, in: Schulz, H.D., Zabel, M. (Eds.), Marine geochemistry. Springer, New York, pp. 311-337.

Smedley, P.L., Kinniburgh, D.G., 2017. Molybdenum in natural waters: A review of occurrence, distributions and controls. Applied Geochemistry 84, 387-432.

Soares, M., 2009. A conceptual model for the responses of mangrove forests to sea level rise. Journal of Coastal Research, 267-271.

Sousa, W.P., Kennedy, P.G., Mitchell, B.J., Ordóñez L, B.M., 2007. Supply-side ecology in mangroves: do propagule dispersal and seedling establishment explain forest structure? Ecological Monographs 77, 53-76.

Sousa, W.P., Mitchell, B.J., 1999. The effect of seed predators on plant distributions: is there a general pattern in mangroves? Oikos 86, 55-66.

Stansell, N.D., Steinman, B.A., Lachniet, M.S., Feller, J., Harvey, W., Fernandez, A., Shea, C.J., Price, B., Coenen, J., Boes, M., 2020. A lake sediment stable isotope record of late-middle to late Holocene hydroclimate variability in the western Guatemala highlands. Earth and Planetary Science Letters 542, 116327.

Stuiver, M., Braziunas, T.F., 1993. Modeling atmospheric 14C influences and 14C ages of marine samples to 10,000 BC. Radiocarbon 35, 137-189.

Toscano, M.A., Macintyre, I.G., 2003. Corrected western Atlantic sea-level curve for the last 11,000 years based on calibrated 14 C dates from Acropora palmata framework and intertidal mangrove peat. Coral Reefs 22, 257-270.

Toth, L.T., Aronson, R.B., Cobb, K.M., Cheng, H., Edwards, R.L., Grothe, P.R., Sayani, H.R., 2015. Climatic and biotic thresholds of coral-reef shutdown. Nature Climate Change 5, 369-374.

Tribovillard, N., Algeo, T.J., Lyons, T., Riboulleau, A., 2006. Trace metals as paleoredox and paleoproductivity proxies: an update. Chemical Geology 232, 12-32.

Urrego, L.E., Bernal, G., Polanía, J., 2009. Comparison of pollen distribution patterns in surface sediments of a Colombian Caribbean mangrove with geomorphology and vegetation. Review of Palaeobotany and Palynology 156, 358-375.

Velez, M.I., Escobar, J., Brenner, M., Rangel, O., Betancourt, A., Jaramillo, A.J., Curtis, J.H., Moreno, J.L., 2014. Middle to late Holocene relative sea level rise, climate variability and environmental change along the Colombian Caribbean coast. The Holocene 24, 898-907.

Ward, R.D., Friess, D.A., Day, R.H., MacKenzie, R.A., 2016. Impacts of climate change on mangrove ecosystems: a region by region overview. Ecosystem Health and Sustainability 2, e01211.

Willard, D.A., Weimer, L.M., Riegel, W.L., 2001. Pollen assemblages as paleoenvironmental proxies in the Florida Everglades. Review of Palaeobotany & Palynology 113, 213-235.

Winter, A., Zanchettin, D., Lachniet, M., Vieten, R., Pausata, F.S., Ljungqvist, F.C., Cheng, H., Edwards, R.L., Miller, T., Rubinetti, S., 2020. Initiation of a stable convective hydroclimatic regime in Central America circa 9000 years BP. Nature Communications 11, 1-8.

Woodring, W.P., 1957. Geology and paleontology of Canal Zone and adjoining parts of Panama. US Government Printing Office, Washington.

Woodroffe, C., 1993. Mangrove sediments and geomorphology, in: Robertson, A.I., Alongi, D.M. (Eds.), Coastal and estuarine studies. American Geophysical Union, Washington DC, pp. 7-43.

Figure captions

Figure 1. Study area. A. Core site location (red star) and geology of Punta Galeta, Caribbean coast of Panama. B and C. Mean monthly precipitation and standard deviation of monthly precipitation (Data from Galeta Meteorological Station from 1974 to 2020; Paton, 2019); months were classified into El Niño, La Niña, and regular conditions, according to the Southern Oscillation Index (SOI) (Ropelewski and Jones, 1987).

Figure 2. Core GAL18 from the mangroves of Punta Galeta, Caribbean coast of Panama. From left to right, photographs of the core, schematization of sediment texture, content of macro rests, and depth-age model. The radiocarbon date in red was excluded from the age-depth model.

Figure 3. The geochemical record of core GAL18 from Punta Galeta, Caribbean coast of Panama. Environmental stages I to V, based on changes in element concentrations, are shown in the column to the right. Indicators are classified according to the interpretation of the record.

Figure 4. Principal component analysis of element concentrations in core GAL18, Caribbean coast of Panama.

Figure 5. The pollen record of core GAL18, Punta Galeta, Caribbean coast of Panama. Taxa are grouped by growing habits (after Marchant et al., 2002), and organized according to depths weighted by taxon abundance; only taxa present in five or more samples are shown; occurrences of *Conocarpus* with abundances below 1% are indicated by asterisks. The last column shows sampling effort, indicating number of pollen and/or spores in each category.

Figure 6. The sedimentary record of Punta Galeta, Caribbean coast of Panama. a) The age-depth model of core GAL18 in the context of the reconstructed sea level for the Caribbean through the last 5200 years; the shaded area is bounded by the estimates of Khan el al. (2017) and Toscano and Macintyre (2003); a modern mean elevation of the coring site of 0.3 m asl is assumed (datum from Sousa et al., 2007). b) Stacked organic and inorganic carbon concentrations of core GAL18. c) Stacked percentages of cf. *Laguncularia*, *Rhizophora*, and *Avicennia*; *Conocarpus* appearances marked by circles. d) PC1 scores of the geochemical record of cores GAL18. e) TOC/TN ratios for core GAL18; the threshold of C/N ratios characteristic of terrestrial vs.

marine organic matter is indicated by the dashed line (after Meyers, 2003); the gray band represents the coral reef growth shutdown reported for Las Perlas archipelago, Panamanian Pacific (Toth et al., 2015). f) Content of sand in El Junco record, Galapagos Islands (Conroy et al., 2008). g) PC1 scores of the geochemical record of cores GAL18. h) Ti content in the Cariaco Basin record (Haug et al., 2001). i) Environmental stages identified in the sedimentary record of Punta Galeta. h) Schematic representation of the evolution of the fringe mangrove of Punta Galeta.

Click here to access/download;Figure;Fig. 1.pdf

Figure 1

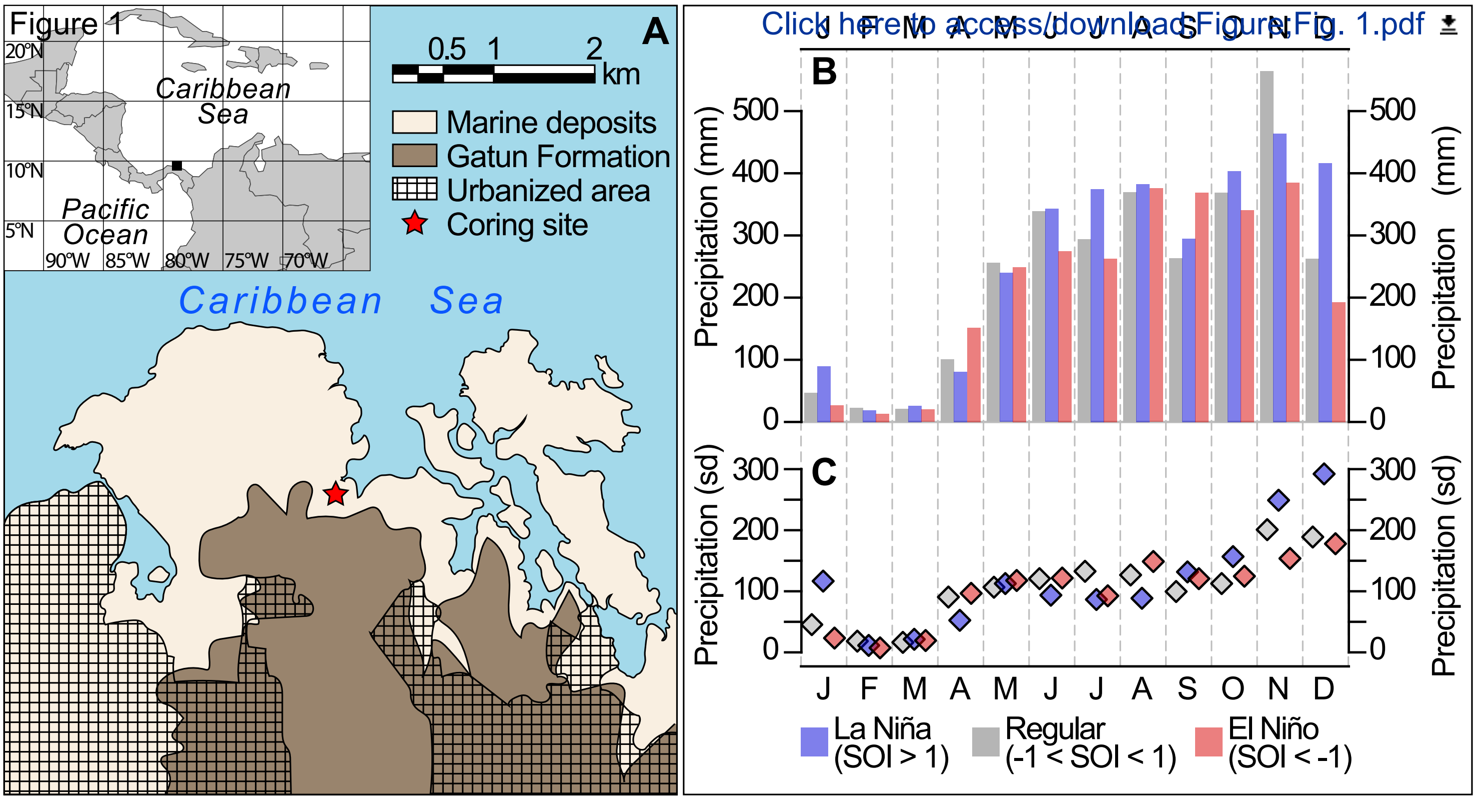

Figure 2

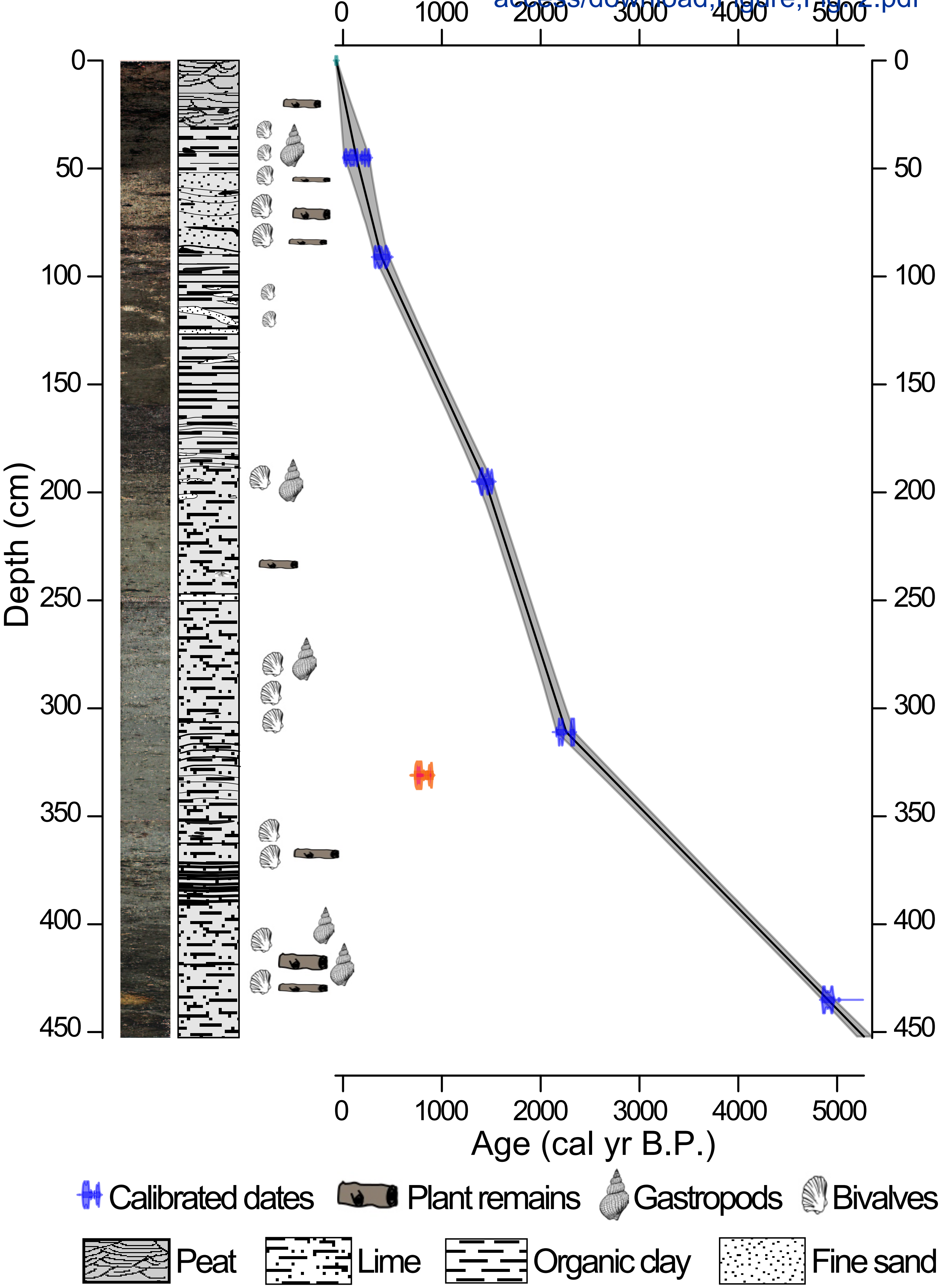

Age (cal yr B.P.)
0
1000
2000
3000
4000
5000
Depth (cm)
0
50
100
150
200
250
300
350
400
450
Calibrated dates
Plant remains
Gastropods
Bivalves
Peat
Lime
Organic clay
Fine sand

Figure 3

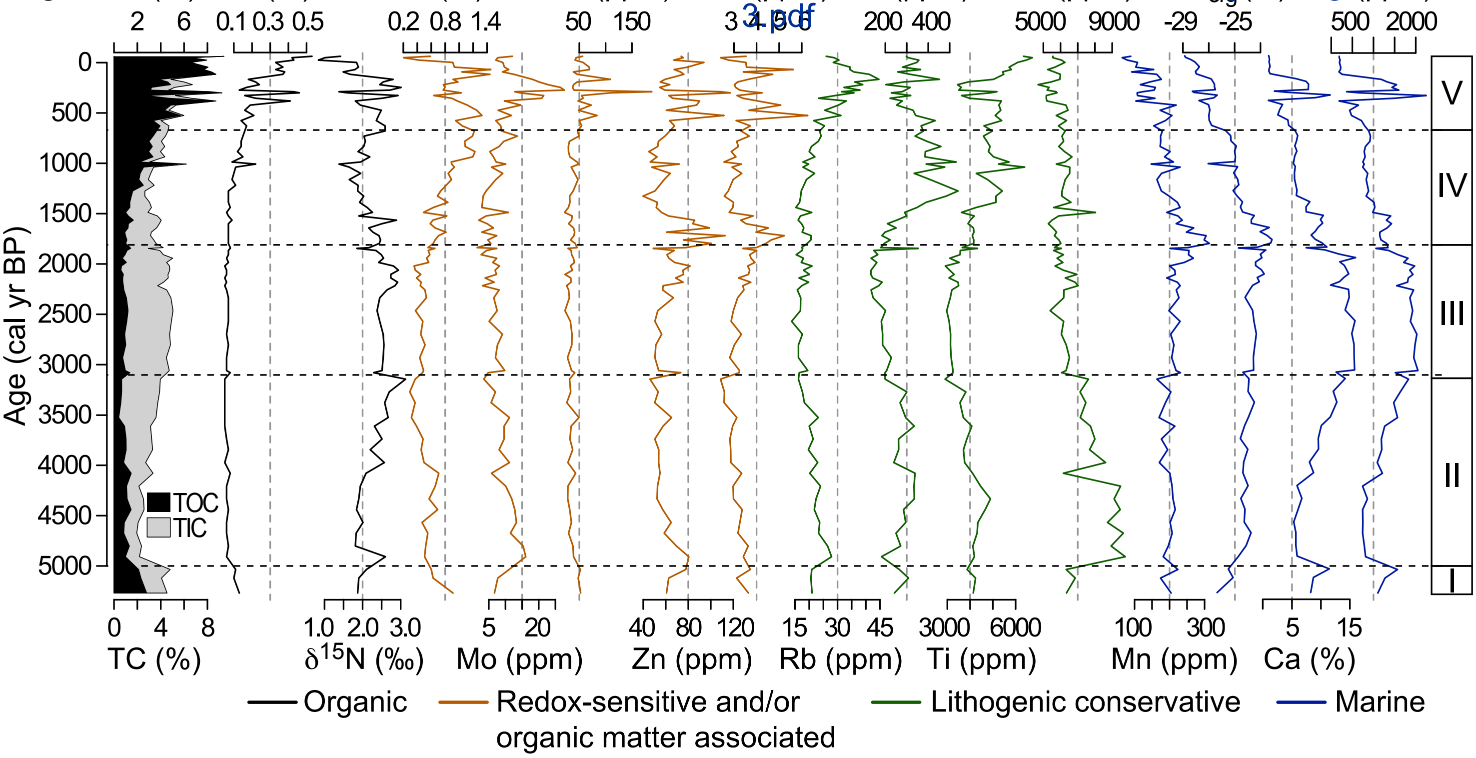
TC (%)
TN (%)
S (%)
Cu (ppm)
Fe (ppm)
Zr (ppm)
K (ppm)
δ13Corg (‰)
Sr (ppm)
Age (cal yr BP)
TOC
TIC
V
IV
III
II
I
TC (%)
δ15N (‰)
Mo (ppm)
Zn (ppm)
Rb (ppm)
Ti (ppm)
Mn (ppm)
Ca (%)
Organic
Redox-sensitive and/or organic matter associated
Lithogenic conservative
Marine

Figure 4

Click here to access/download;Figure;

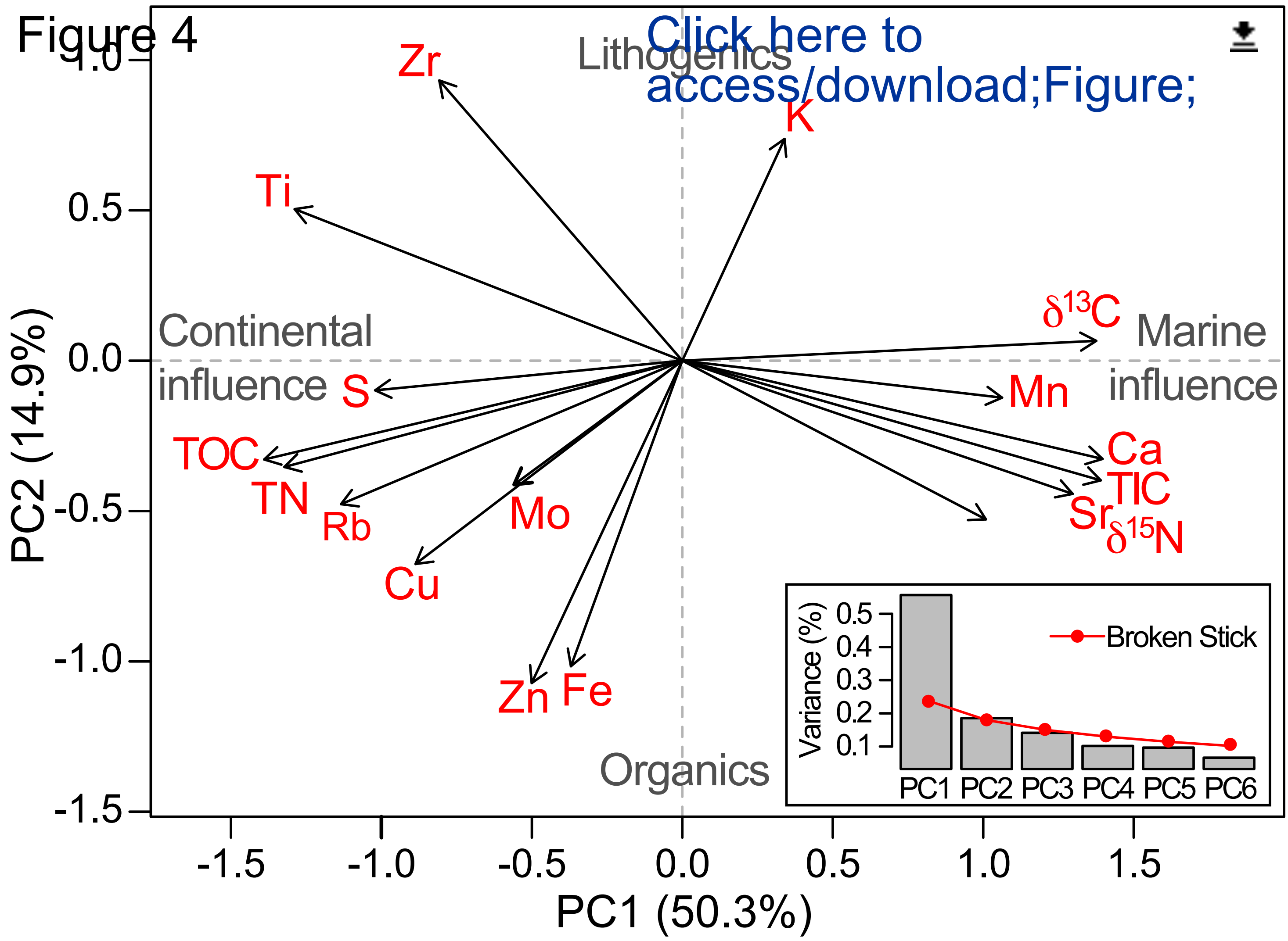

Figure 5

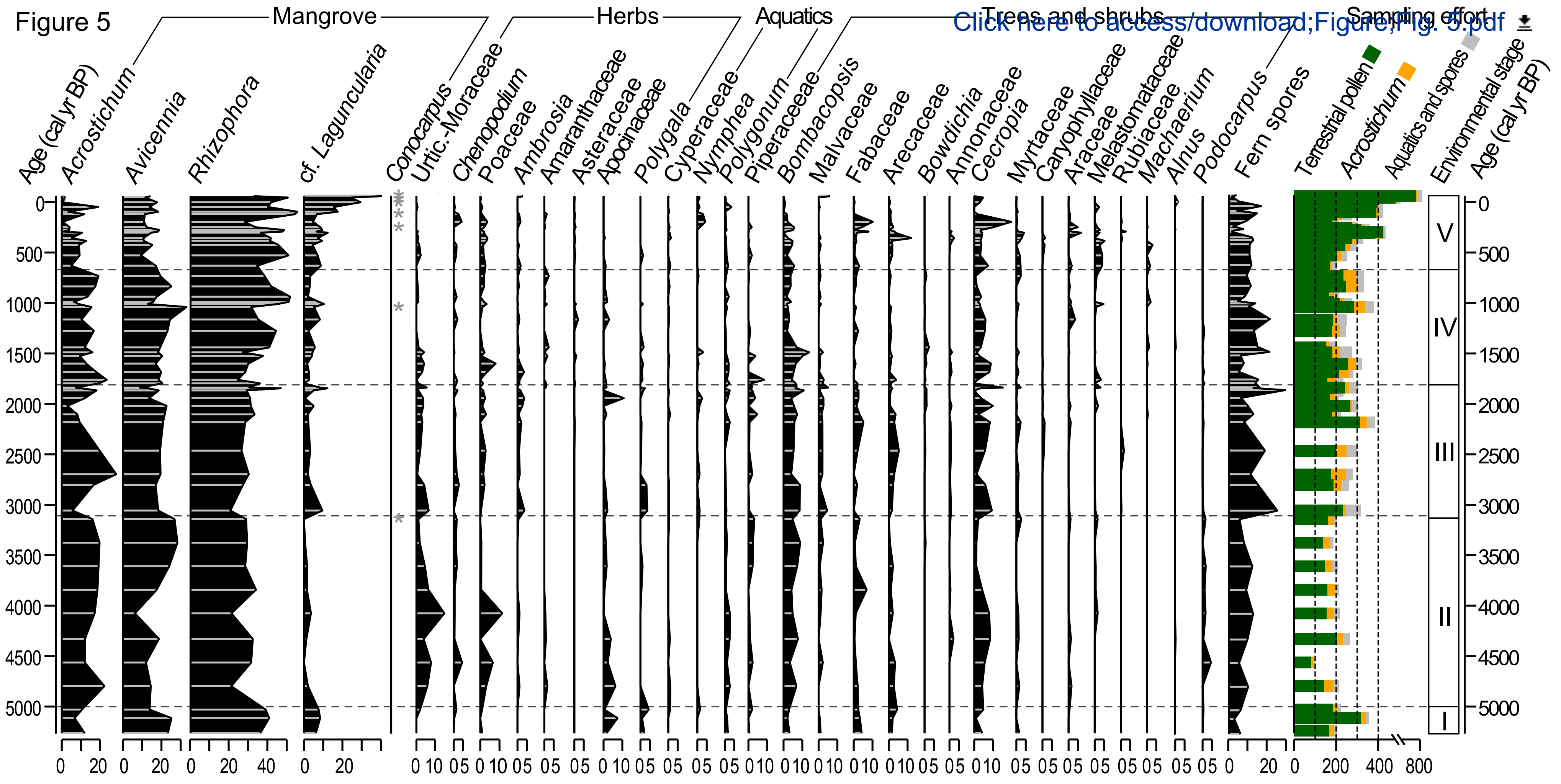
Mangrove
Herbs
Aquatics
Trees and shrubs
Sampling effort
Age (cal yr BP)
Acrostichum
Avicennia
Rhizophora
cf. Laguncularia
Conocarpus
Urtic.-Moraceae
Chenopodium
Poaceae
Ambrosia
Amaranthaceae
Asteraceae
Apocinaceae
Polygala
Cyperaceae
Nymphea
Polygonum
Piperaceeae
Bombacopsis
Malvaceae
Fabaceae
Arecaceae
Bowdichia
Annonaceae
Cecropia
Myrtaceae
Caryophyllaceae
Araceae
Melastomataceae
Rubiaceae
Machaerium
Alnus
Podocarpus
Fern spores
Terrestrial pollen
Acrostichum
Aquatics and spores
Environmental stage
Age (cal yr BP)
V
IV
III
II
I

Figure 6 Click here to access/download;Figure;Fig. 6.pdf